

# Study on A High Voltage Gain SEPIC-Based DC-DC Converter with Continuous Input Current for Sustainable Energy Applications

Hossein Ardi and Ali Ajami

**Abstract**— A high step-up DC-DC converter is proposed in this paper. The presented converter benefits from some advantages such as high voltage gain and continuous input current which makes it suitable for the renewable energy applications. The presented converter is based on the Sepic converter. However, the converter voltage gain is improved by employing a coupled inductor and two voltage multipliers. A passive clamp circuit is also added to the proposed converter which increases the voltage gain and reduces the voltage stress on the main switch. Thus, a switch with low  $R_{DS(on)}$  will be needed which decreases the conduction loss. Besides, the voltage stress on the output diode in the proposed converter is reduced which alleviates reverse recovery problem. The steady state analysis of the proposed converter is discussed in this paper. The analysis is verified with experimental results under the output power of 245 W.

**Index Terms**— DC-DC converter, High voltage gain, voltage multiplier.

## I. INTRODUCTION

NOWADAYS, DC/DC converters are widely employed in various fields of industries. The renewable energy deployment such as photovoltaic panels (PVs) or fuel cells (FCs), DC distribution networks in data centers or electric vehicle (EV) charging stations and battery storage systems in uninterruptable power supplies (UPS) are just some examples for DC/DC converters applications [1]. Renewable energy sources such as PV and F.C. have low DC output voltage. Thus, high step-up DC-DC converter should be used in these systems [2]. Moreover, in order to track the maximum power point in these systems, the input current of the converter should be continuous with low ripple. Thus, the

continuous low ripple input current is very essential for proper input power regulation [3].

In renewable energy systems, when galvanic isolation is not required, the conventional boost converter appears as the first choice. However, extreme duty ratio and consequently low efficiency are the main drawbacks at high output voltage gain [4-6]. Recently, several DC/DC converters have been proposed to increase the output voltage gain.

Switched inductors and switched capacitors structures are common as well [7-9]. The current stress on the main power devices is high in switched inductor structures while the high voltage stress is the main problem in switched capacitor based circuits [10]. Coupled inductor based boost converters are proposed to solve the aforementioned problems [12-22]. The leakage current of the coupled inductor is restored via active or passive clamps. Single switch coupled inductor based converters are also proposed in the literature. Since the leakage inductor of coupled inductors is very low, the input current is pulsating with an undesirable current ripple. The peak current of the leakage inductor passes through the main power switch which deteriorates the overall efficiency. In addition, continuity of the input current causes the RMS value of the input inductor and the switch currents to be reduced which increases the efficiency [6], [10]. By cascading boost converters, high output voltage gain can be achieved. However, too many components will be used in the circuit structures which increase the complexity of the circuit and decrease the total efficiency. Some other Sepic based converters are also presented recently [3], [6], [10]. However, these converters have low voltage gain.

In this paper, a novel high step-up continuous input current DC/DC converter is proposed. The presented converter benefits from numerous advantages such as high output voltage gain, low ripple continuous input current and lower voltage stress. The presented converter consists of a coupled-inductor, an inductor and an improved voltage multiplier cell. The circuit configuration of the proposed converter is shown in Fig. 1. As shown in this picture, capacitors  $C_3$  and  $C_4$  are charged by both sides of the coupled inductor. In conventional voltage multipliers, the capacitors are charged with the secondary side of the coupled inductor. Besides, the voltage stress on the output diode in the proposed converter is less

Manuscript received November 09, 2017; revised December 28, 2017; accepted February 22, 2018.

Hossein Ardi is with the Electrical Engineering Department, Faculty of Engineering, Azarbaijan Shahid Madani University, Tabriz 5375171379, Iran (corresponding author to provide phone: +989146112798; e-mail: ardi@azaruniv.edu).

Ali Ajami is with Research Institute of Applied Power System Studies, Azarbaijan Shahid Madani University, Tabriz, Iran. (e-mail: ajami@azaruniv.edu)

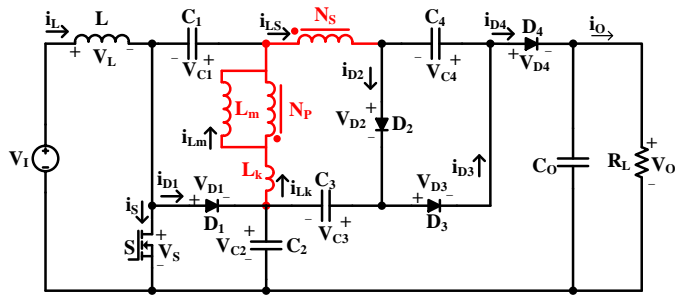


Fig. 1. The circuit prototype of the proposed converter

than other recently-proposed converters which helps solving reverse recovery problem. The voltage across the main switch is clamped by diode  $D_1$  and capacitor  $C_1$ . This causes a switch with low on-resistance  $R_{DS(on)}$  to be used in this converter which reduces the conduction loss. The operation principle of the proposed converter under steady state condition is discussed in the next section.

## II. OPERATING PRINCIPLE OF THE PROPOSED CONVERTER

In order to simplify the operation principle analysis, it's assumed that: 1) all capacitors are large enough without any ripple in their voltages, all inductor  $L$  and  $L_m$  large enough without any ripple in their currents, 2) all components are ideal. The operation principle of the proposed converter in Continuous Conduction Mode (CCM) consists of five time intervals. The current flow path of the proposed converter in different modes and some waveforms of the components are depicted in Fig.2 and Fig. 3, respectively. The steady-state analysis of the presented converter is discussed as follows:

**Mode I** [ $t_0 < t < t_1$ ]: In this time interval, the switch is turned on. Diodes  $D_2$  and  $D_4$  are also on. The current of the leakage inductor is increased rapidly. The current equation of the leakage inductor is:

$$i_{Lk} = \frac{1}{L_k} \int_{t_0}^{t_1} \left( V_{C2} - V_{C1} + \frac{V_o - V_{C1} - V_{C4}}{n} \right) dt \quad (1)$$

Where  $n$  is the turn ratio of the coupled inductor ( $n = N_s/N_p$ ).

The voltage across the leakage inductor is high and also its inductance is very low. Thus, the slope of this current will be high. Therefore, this time interval is too small.

The secondary side current of the coupled inductor reaches zero when the currents of leakage and magnetizing inductor become equal. At this time, diodes  $D_2$  and  $D_4$  are turned off and this mode ends. By applying Kirchhoff Current Law (KCL), the switch current can be obtained as follow:

$$i_S = i_L + i_{Lk} - i_{Ls} \quad (2)$$

**Mode II** [ $t_1 < t < t_2$ ]: In this time interval, the switch is on. As aforementioned, this mode begins when the currents of leakage and magnetizing inductor become equal. Thus, secondary side current of the coupled inductor reaches zero and diodes  $D_2$  and  $D_4$  are turned off. Once the current of the leakage inductor becomes more than the magnetizing inductor current, the direction of the secondary side current of the coupled inductor changes and turns diode  $D_3$  on. Inductor  $L$  is charged by the input source. The magnetizing and leakage

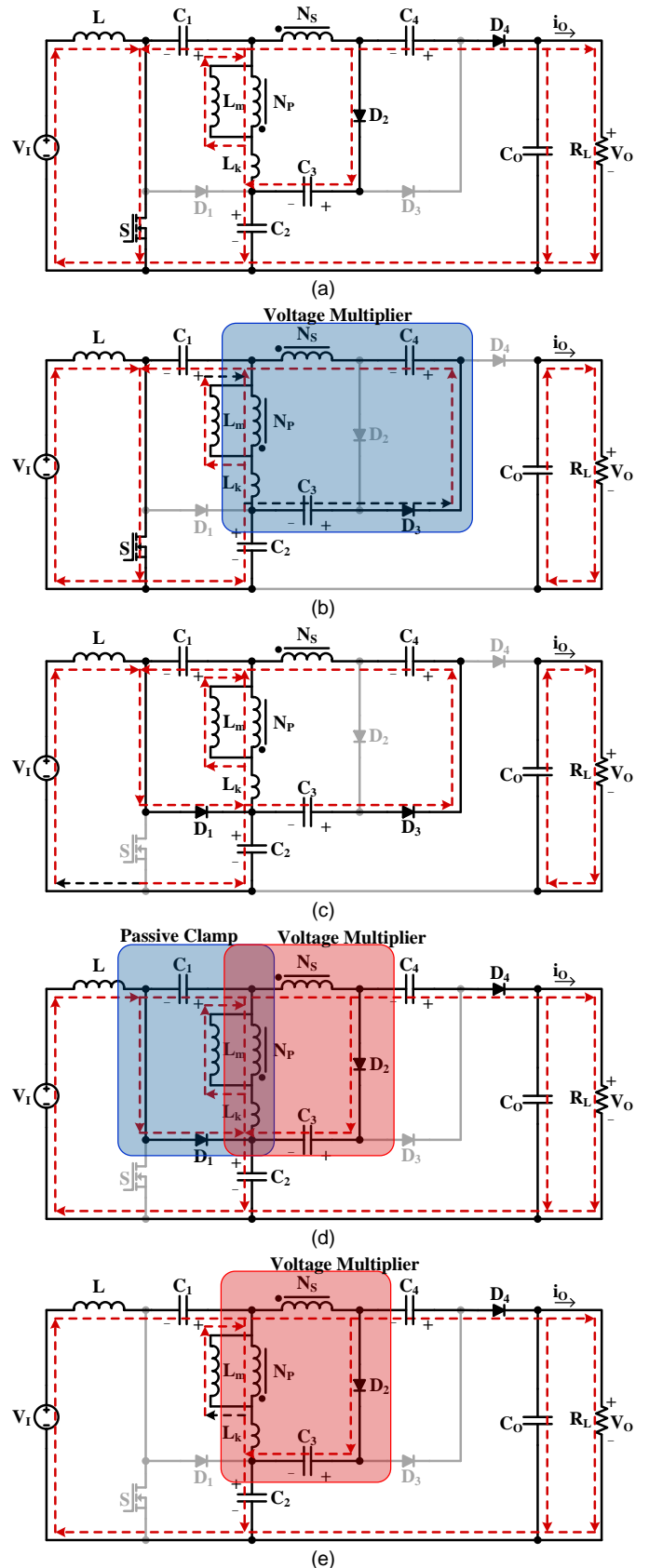


Fig. 2. Current-flow path of operating modes during one switching period at CCM operation. (a) Mode I. (b) Mode II. (c) Mode III. (d) Mode IV. (e) Mode V.

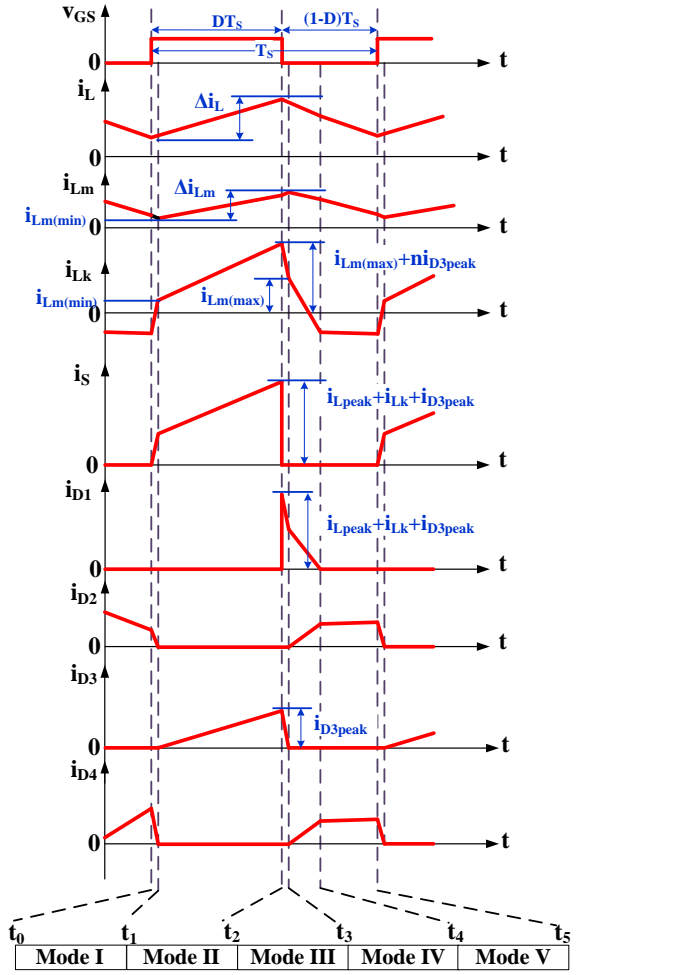


Fig. 3. Some typical waveforms of the proposed converter at CCM operation.

inductors and capacitor  $C_1$  are charged by the energy stored in capacitor  $C_2$ . Capacitor  $C_3$  and secondary side current of the coupled inductor charge capacitor  $C_4$ .

In this mode, the voltage of capacitor  $C_4$  is equal to sum of capacitor voltage  $V_{C4}$  and both sides of the coupled inductor. The output capacitor provides energy to the load. This mode ends by turning the switch off. The following equation can be written for the capacitors currents.

$$\begin{cases} i_{C1} = -i_{C2} = (n+1)i_{D3} + i_{Lm} \\ i_{C4} = -i_{C3} = i_{D3} \end{cases} \quad (3)$$

By applying Kirchhoff Voltage Law (KVL) on the circuit, the following equations can be obtained.

$$V_L = V_I \quad (4)$$

$$V_{Lm} = V_{C2} - V_{C1} - V_{Lk2} \quad (5)$$

$$V_{C4} = V_{C3} + (n+1)(V_{C2} - V_{C1}) \quad (6)$$

Where,  $V_{Lk2}$  is the voltage across the leakage inductor  $L_k$  in mode II. The equation of the leakage inductor current can be written as follows:

$$V_{Lk2} = \frac{(i_{Lk}(t_2) - i_{Lk}(t_1))}{DT_s} L_K, \quad i_{Lk} = ni_{D3} + i_{Lm} \quad (7)$$

**Mode III** [ $t_2 < t < t_3$ ]: In this time interval, the switch is turned

off. The current of inductor  $L$  flows through diode  $D_1$  and charges capacitor  $C_2$ . The currents of diodes  $D_1$  and  $D_3$  can be written as follows:

$$i_{D1} = i_L + i_{Lk} - i_{Ls} \quad (8)$$

$$i_{D3} = -i_{Ls} \quad (9)$$

Where,

$$i_{Ls} = \frac{i_{Lm} - i_{Lk}}{n} \quad (10)$$

In this mode, the leakage inductor is demagnetized. Thus, the energy stored in the leakage inductor is recycled to capacitor  $C_1$  through diode  $D_1$ . The following equation can be written for the leakage inductor:

$$i_{Lk} = \frac{1}{L_K} \int_{t_0}^{t_1} \left( \frac{V_{C3} - V_1 - V_{C4}}{n} - V_{C1} \right) dt \quad (11)$$

Because of high negative voltage across the inductor and low value of inductance, its current slope to be high and so causes this mode like mode I to be too small.

**Mode IV** [ $t_3 < t < t_4$ ]: In this time interval, diodes  $D_1$ ,  $D_2$  and  $D_4$  are on. Recycling the energy of the leakage inductor is continued in this mode too. Once the leakage inductor current become smaller than the magnetizing inductor current, according to (9), the direction of the secondary side current of the coupled inductor is changed and turns diode  $D_2$  and  $D_4$  on. The capacitor currents in this mode can be found as follows:

$$\begin{cases} i_{C1} = -(I_L - i_{D1}) \\ i_{C4} = -i_{D4} = i_{C2} - I_L = -i_{C0} - I_O \\ i_{C3} = i_{D2} \end{cases} \quad (12)$$

Moreover, the following equation can be written for the currents of diodes  $D_1$ ,  $D_2$  and  $D_4$  in this mode.

$$i_{D1} = i_L + i_{Lm} - (n+1)(i_{D2} + i_{D4}) \quad (13)$$

In conventional voltage multipliers, just the secondary side of the coupled inductors become in parallel with the capacitors. However, as seen in Fig. 2(d), in the proposed converter, both sides of the coupled inductor become in parallel with capacitor  $C_3$ . This makes the voltage across capacitor  $C_3$  and as a result, the voltage gain to be increased. The voltage of capacitors in this mode can be found as follows:

$$V_L = V_I - V_{C2} \quad (14)$$

$$V_{Lm} = -V_{C1} - V_{Lk4} \quad (15)$$

$$V_O = V_{C2} + V_{C3} + V_{C4} \quad (16)$$

$$V_{C3} = (n+1)V_{C1} + nV_{Lk4} \quad (17)$$

Where  $V_{Lk4}$  is the voltage across the leakage inductor in mode IV which can be found as follow:

$$V_{Lk4} = \frac{(i_{Lk}(t_4) - i_{Lk}(t_3))}{d_4 T_s} L_K, \quad i_{Lk} = -ni_{D2} + i_{Lm} \quad (18)$$

Where,  $d_4 T_s$  is time interval of mode IV.

**Mode V** [ $t_4 < t < t_5$ ]: This is the last time interval for a switching period. The energy of the leakage inductor has been

recycled to capacitor  $C_2$  in modes III and IV. The energy of inductors and the input source charge the output capacitor and provide energy to the load through diode  $D_4$ . Diode  $D_2$  is still on and capacitor  $C_3$  is parallel with both sides of the coupled inductor. Applying KCL in this mode, yields:

$$i_{D2} = i_{D4} = i_{Ls} = \frac{i_{Lm} + i_L}{n+1}, i_{Lk} = \frac{i_{Lm} - ni_L}{n+1} \quad (19)$$

It's worth noting that by neglecting current ripples of inductors  $L$  and  $L_m$ , the current slope of leakage inductor and diodes  $D_2$  and  $D_4$  are almost zero. Thus, the voltage across the leakage inductor in this mode is zero. It's worth noting that by assuming that the capacitors are large, the currents of diodes  $D_2$  and  $D_4$  are equal. The following equations can be achieved in this mod.

$$V_{Lm} = \frac{-V_{C3}}{n+1} = -V_{C1} - \frac{n}{n+1}V_{Lk4} \quad (20)$$

$$V_L = V_I - V_{C2} - \frac{n}{n+1}V_{Lk4} \quad (21)$$

By applying volt-second balance principle on the inductor voltages, the following equations can be obtained.

$$V_{C1} = \frac{DV_I}{1-D} - DV_{Lk2} - \quad (22)$$

$$\left(\frac{n}{1+n}\right)\left(d_4 + \frac{(1-D-d_4)}{(1-D)}\right)V_{Lk4}$$

$$V_{C2} = \frac{V_I}{1-D} - \frac{n(1-D-d_4)}{(n+1)(1-D)}V_{Lk4} \quad (23)$$

Neglecting modes I and III and by applying volt-second balance principle on the inductor  $L_k$ , the following equation is obtained.

$$DT_S V_{Lk2} + d_4 T_S V_{Lk4} + 0 = 0 \Rightarrow V_{Lk2} = -\frac{d_4}{D} V_{Lk4} \quad (24)$$

Using equations (6), (16), (17), (22), (23) and (24) the output voltage of the proposed converter can be obtained as follows:

$$V_O = MV_I + \left((n+1)(d_4 + D) + \frac{n}{n+1}(Md_4 - (1-D))\right)V_{Lk4} \quad (25)$$

Where  $M$  is the voltage gain of the proposed converter by neglecting the leakage inductor ( $L_k=0$ ,  $V_{Lk4}=0$ ). The value of  $M$  is:

$$M = \frac{n+2+D(n+1)}{1-D} \quad (26)$$

This equation can be found by using equations (6), (16), (17), (22) and (23) and also by considering the leakage inductor and its voltages to be zero. In order to find the voltage gain of the proposed converter without neglecting leakage inductance, the  $V_{Lk2}$  and  $V_{Lk4}$  should be found. By applying ampere-second balance principles on the capacitors, it can be proved that the average values of diode currents are equal to the output current. According to Fig. 3, the average values of diode  $D_3$  can be achieved.

$$\langle i_{D3} \rangle = I_O \Rightarrow Di_{D3peak} = 2I_O \Rightarrow i_{D3peak} = \frac{2I_O}{D} \quad (27)$$

Neglecting the leakage inductor and power loss yields:

$$I_L = MI_O \quad (28)$$

Applying ampere-second balance principle on capacitor  $C_1$ , the average value of  $I_{Lm}$  can be found.

$$\langle i_{C1} \rangle = DI_{Lm} + (n+1)I_O + I_O - DI_L = 0 \quad (29)$$

$$\Rightarrow I_{Lm} = (n+1)I_O$$

The value of  $d_4$  can be found as follows:

$$\begin{aligned} \langle i_{D1} \rangle = I_O &= \frac{(I_L + I_{Lm})d_4 T_S}{2T_S} \\ &= \frac{(M + (n+1))d_4 I_O T_S}{2T_S} \Rightarrow d_4 = \frac{2(1-D)}{2n+3} \end{aligned} \quad (30)$$

Substituting (27) into (7) and using equation (24), the value of  $V_{Lk4}$  can be obtained as follows:

$$V_{Lk4} = -\frac{n(2n+3)Q}{D(1-D)}V_O, Q = \frac{f_S L_K}{R_L} \quad (31)$$

The voltage of capacitors  $C_3$  and  $C_4$  and the voltage gain can be found as well.

$$V_{C3} = \frac{(n+1)D}{1-D}V_I + \left[n + \frac{2D+1-2n}{(2n+3)}\right]V_{Lk4} \quad (32)$$

$$V_{C4} = \frac{(n+1)}{1-D}V_I + \left[n + \frac{4D-1-2n}{(2n+3)} + \frac{2n(1-D)}{D(2n+3)}\right]V_{Lk4} \quad (33)$$

$$G_{CCM} = \frac{MD^2(1-D)}{D^2(1-D) - 2[A]nQ} \quad (34)$$

$$A = D^2(2n^3 + 9n^2 + 10n + 2) + nD(2n+6) - n$$

Where,  $G_{CCM}$  is the voltage gain of the proposed converter. According to equation (34), if  $L_k=0$ , the value of  $Q$  will be zero and the voltage gain will be equal to equation (26).

### III. CONVERTER DESIGN CONSIDERATION

In order to operate a converter properly, its components should be designed appropriately. Therefore, design of the components for the proposed converter is discussed here. Since operating in Discontinuous Conduction Mode (DCM) has some disadvantages such as slow dynamic response, dependence on frequency the output power and the value of inductors and also high current stress on the semiconductors, the proposed converter should be designed to operate under CCM condition. According to [9], [23], [24], if the average current value of the inductor is more than half of its ripple, the converter will operate in CCM. The current ripple of inductors  $L$  and  $L_m$  can be obtained using integral formula of inductors.

$$\Delta i_L = \frac{DV_I}{Lf_S} \quad (35)$$

$$\Delta i_{Lm} = \frac{DV_I}{L_m f_S} \quad (36)$$

Therefore, the minimum value of inductor  $L$  in order to operate in CCM can be achieved as follows:

$$L \geq \frac{DR_L}{2M^2 f_S} \quad (37)$$

In order to operate the proposed converter in CCM, the value of  $L_m$  is also should be calculated and designed properly. If the proposed converter operates in Boundary Conduction Mode (BCM), at the end of the switching period, the inductor currents  $i_L$  and  $i_{Lm}$  will be equal. Thus:

$$i_{L \min} = -i_{Lm \min} \Rightarrow I_{Lm} - \frac{\Delta i_{Lm}}{2} = \frac{\Delta i_L}{2} - I_L \quad (38)$$

Therefore, if the following inequality is valid, the proposed converter will operate in CCM.

$$i_{L \min} = -i_{Lm \min} \Rightarrow I_{Lm} - \frac{\Delta i_{Lm}}{2} \geq \frac{\Delta i_L}{2} - I_L \quad (39)$$

Using equations (28), (29), (35), (36) and (39), the minimum value of inductor  $L_m$  can also be calculated using the following equation:

$$L_m \geq \frac{2L(1-D)R_L}{2D(1-D)R_L - 4(2n+3)f_s ML} \quad (40)$$

Ignoring the ESR of capacitors, the voltage ripple of the output capacitor can be found as follows:

$$V_{Co}(DT_s) = V_{Co}(0) + \frac{1}{C_o} \int_0^{DT_s} i_{Co}(t) dt \quad (41)$$

$$\Rightarrow \Delta V_{Co} = \frac{DV_o}{f_s R_L C_o}$$

Using this equation and considering certain voltage ripple, the output capacitor value can be found.

According to Fig. 2, the voltage stress on the semiconductors can be written as follows:

$$V_{D1} = V_S = V_{C2} = \frac{V_I}{1-D} \quad (42)$$

$$V_{D2} = V_{D3} = V_{D4} = V_{C4} = \frac{(n+1)V_I}{1-D} \quad (43)$$

The current stress on diode  $D_3$  is calculated in equation (27). The current stress on the switch and diodes can be achieved as follows:

$$i_{Speak} = i_{D1peak} = i_L + i_{Lk} + i_{D3} = \left( \frac{2(n+1)}{D} + \frac{2n+3}{1-D} \right) I_o \quad (44)$$

$$I_o = \frac{(2(1-D)-d_4)i_{D2,4peak}}{2} \Rightarrow i_{D2,4peak} = \frac{(2n+3)I_o}{2(n+1)(1-D)} \quad (45)$$

#### IV. COMPARISON STUDY

In this session, some comparisons between the suggested converter and other recently-proposed converters are presented. The specifications of the converters are compared in Table I. The voltage gain and voltage stress on the main switch are compared in Fig. 4 and Fig. 5, respectively. The proposed converter has continuous and low-ripple input current. Thus it will be more suitable for renewable energy applications.

For instance, in some applications such as fuel cell (F.C.) which has slow dynamic response, the converters which have high input current ripple cannot operate properly. In order to solve this problem, an input filter is required which increase the number of components. The voltage gain of the proposed converter and some other recently-proposed converters are compared in Fig. 4. As shown in this figure, the voltage gain of the presented converter is higher than other converters. Besides, the voltage stress on the main switch in the proposed converter is lower than other converters. Comparing Fig. 4 and Fig. 5 yields that the voltage stress on the switch for the converter with higher voltage gain is less than the others.

#### V. EXPERIMENTAL RESULTS

In order to validate the theoretical analysis and justify the feasibility of the proposed converter, the experimental results of implemented circuit of the proposed converter are analyzed in this session. The specifications of the implemented prototype are given in Table II. The proposed converter increases the input voltage of 20V to output voltage of 300V at the output power of 245W. The voltage of capacitors and semiconductors and the currents of inductor and semiconductors are shown in Fig. 6. The time per division in the figures is 10 $\mu$ s. Under this condition and according to equations (37) and (40), the minimum values of inductors can be calculated to operate the converter in CCM.

Table I. The comparison between the proposed converter and some other converters.

Reference	Number of Components				Voltage Stress on Switch	Voltage Gain	Current Stress on Switch	$\sum V_D$
	diode	switch	capacitor	core				
Proposed Converter	4	1	4	2	$\frac{M+n+1}{2n+1}V_I$	$\frac{n+2+(n+1)D}{1-D}$	$\left( \frac{2(n+1)}{D} + \frac{2n+3}{1-D} \right) I_o$	$\frac{(3n+5)(M+n+1)}{2n+1}V_I$
Converter in [10]	3	1	3	2	$\frac{M}{n+2}V_I$	$\frac{n+2}{1-D}$	$M I_o + \left( \frac{2(n+1)}{D} \right) I_o$	$\frac{M(2n+3)}{n+2}V_I$
Converter in [3]	3	1	3	2	$\frac{M}{n+1}V_I$	$\frac{n+1}{1-D}$	$\left( \frac{2nM}{M-n-1} + M \right) I_o$	$\frac{M(2n+1)}{n+1}V_I$
Converter in [11]	4	1	3	1	$\frac{M-n}{n+1}V_I$	$\frac{n+1+nD}{1-D}$	$\left( \frac{(2n+1)(M-n)}{1+n} + \frac{2n(M-n)}{M-2n-1} \right) I_o$	$\frac{(M-n)(3n+1)}{n+1}V_I$
Converter in [9]	4	1	3	1	$\frac{M+n}{2(n+1)}V_I$	$\frac{n+2+nD}{1-D}$	$\frac{M(M+n)}{M-n-2}I_o$	$\frac{3}{2}(M+n)V_I$

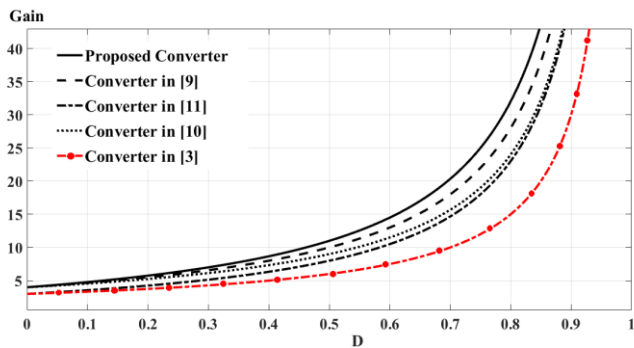


Fig. 4. The voltage gain of the suggested converter and the proposed converters in [3], [9], [10] and [11] ( $n=2$ )

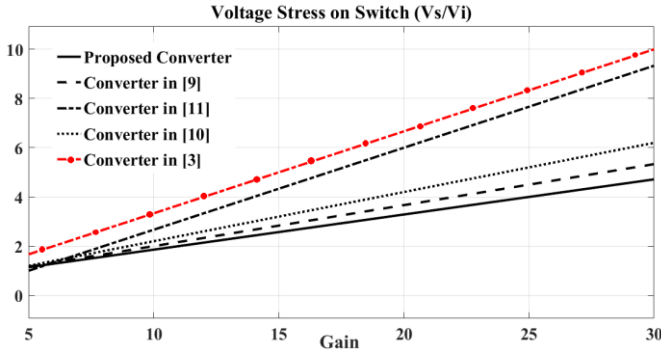


Fig. 5. The voltage stress on the main switch for the suggested converter and the proposed converters in [3], [9], [10] and [11] ( $n=2$ ).

However, in this condition, the converter will operate near DCM which is caused the current ripples and stresses to be high. Thus, in order to design the inductors properly, the current ripples are considered to be less than 10% of their average. According to equations (35) and (36), the value of

inductor  $L$  is chosen  $320\mu\text{H}$ . The value of  $L_m$  can also be chosen as well.

For the voltage gain calculation, some assumptions are considered to simplify the analysis. For instance, the voltage forward of the diodes and resistances of components are neglected. Thus the calculated voltage gain of the proposed converter will be different from the measured voltage gain. However, considering them does not increase the duty ratio very much. According to equation (34), the duty ratio of the proposed converter for the input and output voltage of 20V and 300V is about 62%. However, according to Fig. 6, the duty ratio of the power switch is about 65%.

As shown in Fig. 6, the input current is about 13.1 A. The output power is 245 W. Therefore, the efficiency of the proposed converter under the output power of 245 W is about 93.5%. The efficiency curve of the proposed converter versus the output power is depicted in Fig. 7.

Table II. The circuit parameters of the implemented prototype.

Specifications	Values
Input Voltage	20V
Output Voltage	300V
Capacitors	$C_1, C_2, C_3, C_4=47\ \mu\text{F}, C_0=180\ \mu\text{F}$
Inductor ( $L$ )	$320\ \mu\text{H}$
Coupled-inductor	$L_m=100\ \mu\text{H}, n=2$
Switching frequency	50kHz
Power Switches	IRFP260
Diodes	MUR1560

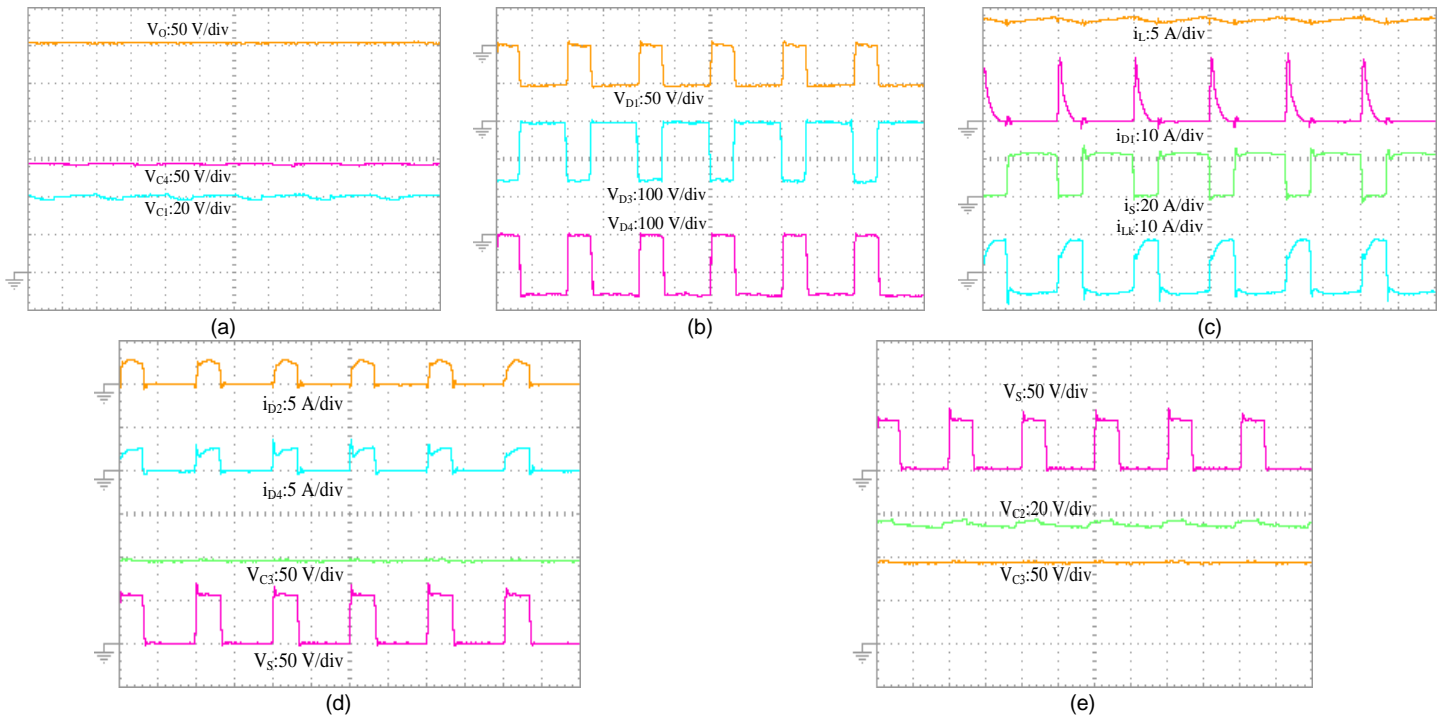


Fig. 6. Experimental results of the proposed converter.



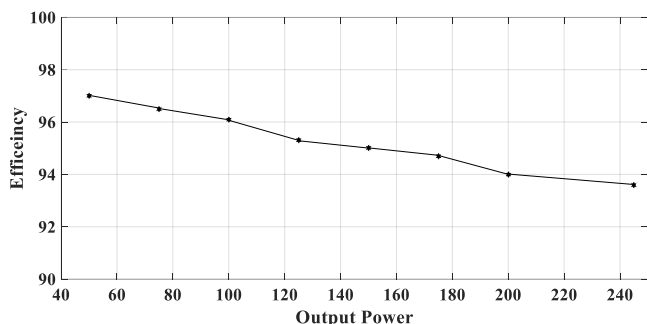


Fig. 7. Efficiency curve of the proposed converter versus various output power.

## VI. CONCLUSION

A high step-up DC-DC converter is studied in this paper. The proposed converter has high voltage gain and continuous and low-ripple input current. A passive voltage clamp and two voltage multipliers are added to the converter to achieve high voltage gain. This cause the number of components to be high. Besides, the power is transferred to the load with some steps from input to output. These causes high conductions in the proposed converter. Since both sides of the coupled inductor charge the capacitors of voltage multipliers, the voltage gain of the proposed converter in comparison other converters with same number of components to be higher. Thus, higher voltage gain can be achieved with low duty ratio. The steady state analysis of the proposed converter is discussed in this paper. The voltage gain, voltage stress on the main switch and also sum of voltage stress on diodes and the current stress on the main switch are compared between the proposed converter and other converters. According to the presented results, the voltage stress on main switch in suggested converter is less than other converters. Finally, the presented topology is implemented experimentally under the output power of 245W in order to justify the theoretical analysis.

## REFERENCES

- [1] H. Ardi, A. Ajami, F. Kardan and S. Nikpour, "Analysis and Implementation of a Non-Isolated Bidirectional DC-DC Converter with High Voltage Gain," *IEEE Trans. Ind. Electron.*, vol. 63, no. 8, pp.4878-4888, Aug. 2016.
- [2] H. Ardi, R. Reza Ahrabi, S. Najafi, "Non-isolated bidirectional DC-DC converter analysis and implementation," *IET Power Electron.*, vol. 5, no. 12, pp.3033-3044, Dec. 2014.
- [3] R. Gules, W. M. d. Santos, F. A. d. Reis, "A Modified SEPIC Converter with High Static Gain for Renewable Applications," *IEEE Trans. Power Electron.*, vol. 29, no. 11, pp. 5860- 5871, Nov. 2014.
- [4] L. S. Yang, T. J. Liang, and J. F. Chen, "Transformer-less DC-DC converter with high voltage gain," *IEEE Trans. Ind. Electron.*, vol. 56, no. 8, pp. 3144-3152, Aug. 2009.
- [5] Y. P. Hsieh, J. F. Chen, T. J. Liang, and L. S. Yang, "Novel high step-up DC-DC converter with coupled-inductor and switched-capacitor techniques," *IEEE Trans. Ind. Electron.*, vol. 59, no. 2, pp. 998-1007, Feb. 2012.
- [6] H. Ardi, A. Ajami, M. Sabahi, "A Novel High Step-up DC-DC converter with Continuous Input Current Integrating

- Coupled Inductor for Renewable Energy Application," *IEEE Trans. Ind. Electron.*, early access, Jul, 2017.
- [7] Y. P. Hsieh, J. F. Chen, T. J. Liang, and L. S. Yang, "Novel high step-up DC-DC converter for distributed generation system," *IEEE Trans. Ind. Electron.*, vol. 60, no. 4, pp. 1473-1482, Apr. 2013.
- [8] S. M. Chen, T. J. Liang, L. S. Yang, and J. F. Chen, "A Boost Converter with Capacitor Multiplier and Coupled Inductor for AC Module Applications," *IEEE Trans. Ind. Electron.*, vol. 60, no. 4, pp.1503-1511, Apr. 2013.
- [9] A. Ajami, H. Ardi, A. Farakhor, "A Novel High Step-up DC/DC converter Based on Integrating Coupled Inductor and Switched-Capacitor techniques for Renewable Energy Applications," *IEEE Trans. Power Electron.*, vol. 30, no. 8, pp. 4255-4263, Aug. 2015.
- [10] R. Moradpour, H. Ardi, A. Tavakoli, "Design and Implementation of a New SEPIC-Based High Step-Up DC/DC Converter for Renewable Energy Applications," *IEEE Trans. Ind. Electron.*, early access, Jul, 2017.
- [11] B. Axelrod, Y. Beck, Y. Berkovich, "High step-up DC-DC converter based on the switched-coupled-inductor boost converter and diode-capacitor multiplier: steady state and dynamics", *IET Power Electron.*, vol. 8, no. 8, pp. 1420-1428, Feb. 2015.
- [12] H. Ardi, A. Ajami, M. Sabahi, "A Sepic based high step-up DC-DC converter integrating coupled inductor for renewable energy applications," *Power Electronics, Drive Systems & Technologies Conference (PEDSTC), 2017 8th. IEEE*, 2017.
- [13] K. C. Tseng and C. C. Huang, "High step-up, high efficiency interleaved converter with voltage multiplier module for renewable energy system" *IEEE Trans. Ind. Electron.*, vol. 61, no. 3, pp. 1311-1319, Mar. 2014.
- [14] I. Laird, and D. D. C. Lu, "High Step-Up DC/DC Topology and MPPT Algorithm for Use with a Thermoelectric Generator," *IEEE Trans. Power Electron.*, vol. 28, no. 7, pp. 3147-3157, Jul. 2013.
- [15] C. L. Wei and M. H. Shih, "Design of a switched-capacitor DC-DC converter with a wide input voltage range," *IEEE Trans. Circuits Syst.*, vol. 60, no. 6, pp. 1648-1656, Jun. 2013.
- [16] S. M. Chen, M. L. Lao, Y. H. Hsieh, T. J. Liang, and K. H. Chen, "A Novel Switched Coupled-Inductor DC-DC Step-Up Converter and Its Derivatives" *IEEE Trans. Ind. Electron.*, vol. 3, no. 4, pp. 309-314, Feb. 2015.
- [17] K. C. Tseng, J T. Lin, and C. C. Huang, "High Step-Up Converter with Three-Winding Coupled Inductor for Fuel Cell Energy Source Applications," *IEEE Trans. power. Electron.*, vol. 30, no. 2, pp. 574-581, Feb. 2015.
- [18] A. Farakhor, H. Ardi, M. Abapour, "Analysis and design procedure of a novel high voltage gain DC/DC boost converter," *Power Electronics, Drive Systems & Technologies Conference (PEDSTC), 2017 8th. IEEE*, 2017.
- [19] T. Nouri, N. Vosoughi, S. H. Hosseini and M. Sabahi, "A Novel Interleaved Nonisolated Ultrahigh-Step-Up DC-DC Converter With ZVS Performance" *IEEE Trans. Ind. Electron.*, vol. 64, no. 5, pp. 3650 - 3661, Jan. 2017.
- [20] T. Nouri, S. H. Hosseini and E. Babaei and J. Ebrahimi, "Generalised transformer-less ultra step-up DC-DC converter

with reduced voltage stress on semiconductors” *IET Power Electron.*, vol. 7, no. 11, pp. 2791 - 2805, Nov. 2014.

[21] J. H. Lee, T. J. Liang, and J. F. Chen, “Isolated coupled-inductor- integrated DC–DC converter with non-dissipative snubber for solar energy applications,” *IEEE Trans. Ind. Electron.*, vol. 61, no. 7, pp. 3337–3348, Jul. 2014.

[22] Y. P. Hsieh, J. F. Chen, T. J. Liang and L. S. Yang, “A Novel High Step-Up DC–DC Converter for a Microgrid System,” *IEEE Trans. Power Electron.*, vol. 26, no. 4, pp.1127- 1136, Apr. 2011.

[23] R. W. Erickson, D. Maksimovic, “Fundamentals of power electronics,” Norwell, Massachusetts: Kluwer (2001, 2nd edn.)

[24] A. Ioinovici, “Power Electronics and Energy Conversion Systems,” vol. 1. Wiley, UK, 2013.



**Hossein Ardi** was born in Miyaneh, Iran, in 1990. He received the B.Sc. degree in electrical engineering and the M.Sc. degree (first-class Hons.) in power electronic engineering from Azarbaijan Shahid Madani University, Tabriz, Iran, in 2012 and 2014, respectively, where he is currently working toward the Ph.D. degree in power electronic engineering at the Faculty of Engineering. He is a Member of Organization Exceptional Talents at the Azarbaijan Shahid Madani University. He was also selected as the best

student researcher at Azarbaijan shahid Madani Univertsity in 2015. His research interests include renewable energies, power electronic converters, especially high-step-up dc-dc converters, and multi-input converters. He is currently focusing on the single-stage multi-input converters.



**Ali Ajami** received his B.Sc. and M. Sc. degrees from the Electrical and Computer Engineering Faculty of Tabriz University, Iran, in Electronic Engineering and Power Engineering in 1996 and 1999, respectively, and his Ph.D. degree in 2005 from the Electrical and Computer Engineering Faculty of Tabriz University, Iran, in Power Engineering. Currently, he is Prof. of electrical engineering department of Azarbaijan Shahid Madani University. His main research

interests are power electronics converters design, modeling and controlling, microprocessors, DSP and computer based control systems, applications of power electronics converters for renewable energy, harmonics and power quality compensation systems and dynamic and steady state modeling and analysis of FACTS devices.